Journal of Applied Polymer Science

Optimization of the Spark Plasma Sintering Processing Parameters Affecting the Properties of Polyimide

Maxime Schwertz,[1,2] Pierre Ranque,[1] Sébastien Lemonnier,[1] Elodie Barraud,[1] Adele Carradò,[3] Marie-France Vallat,[2] Michel Nardin[2]

[1]French-German Research Institute of Saint-Louis, 5, rue du Général Cassagnou, 68300 Saint-Louis, France
[2]Institut de Science des Matériaux de Mulhouse UMR 7361 CNRS UHA, Université de Haute-Alsace, 68057 Mulhouse, France
[3]Institut de Physique et Chimie des Matériaux de Strasbourg UMR 7504 CNRS UdS, Université de Strasbourg, 67034 Strasbourg, France
Correspondence to: M. Schwertz (E-mail: maxime.schwertz@isl.eu)

ABSTRACT: The present study deals with the optimization of polyimide (PI) mechanical properties, obtained by Spark Plasma Sintering (SPS), by using a method combining Design of Experiments (DOE) with physical, structural, and mechanical characterizations. The effects of SPS parameters such as temperature, pressure, dwell time, and cooling rate on the density, mechanical properties, and structure of PI were investigated. The experimental results revealed that the mechanical properties of the material were optimized by raising the sintering temperature up to 350°C. The optimized SPS processing parameters were a temperature of 350°C, a pressure of 40 MPa, and a dwell time of 5 min. Under these conditions, a relative density of 99.6% was reached within only a few minutes. The corresponding mechanical properties consisted of Young's modulus of 3.43 GPa, a Shore D hardness of 87.3, and a compressive strength of 738 MPa for a maximum compressive strain of 61.8%. Moreover, when working at 320°C and at 100 MPa, an increase in the dwell time was necessary to enhance the properties. Contrary to the other parameters, the cooling rate appeared to be a non-significant parameter. Finally, correlations between the PI structure and the mechanical properties were made to demonstrate the densification mechanisms. © 2014 Wiley Periodicals, Inc. J. Appl. Polym. Sci. **2015**, *132*, 41542.

KEYWORDS: mechanical properties; structure–property relations; polyimide; spark plasma sintering; design of experiments

Received 6 August 2014; accepted 19 September 2014
DOI: 10.1002/app.41542

INTRODUCTION

High-performance polymers, such as polyimide (PI), have aroused considerable attention in the last few decades, due to their outstanding properties such as high strength, light weight, excellent thermal stability, combined with wear and solvent resistance.[1,2] PI materials are largely used in aerospace, microelectronics, or automotive industries as high-temperature composites, adhesives, dielectrics, photoresists, nonlinear optical, and membrane materials.[2,3] In particular, they have found a number of applications in mechanical engineering as structural materials.[2–5]

Usually, thermoplastic PIs are synthesized in the form of films on account of their ease of processing, handling, and storage.[3,6–12] This PI synthesis consists of two steps. Firstly, a solution of polyamic acid (PAA) is prepared by condensation of a dianhydride and a diamine in a polar aprotic solvent such as *N*-methyl-2-pyrrolidone (NMP).[1–3] Secondly, the PAA solution is deposited by using different methods (spinning, dipping, or casting) on substrates (glass, silicon wafers). A thermal treatment is used to remove the solvents and convert the PAA into PI. The disadvantages of this method are, on one hand, the inevitable presence of solvents and the necessity of removing them by evaporation, causing extensive film shrinkage. On the other hand, this method cannot be used for the preparation of uniform thick films on substrates or large pieces with complex geometries.[1–3] To obtain such pieces without solvent evaporation during the processing stage, an alternative "dry" method applying the powder consolidation technique was reported in the literature,[4,5,13–28] as summarized in Table I. The PAA is dried directly after its synthesis to obtain a powder which will be consolidated by sintering.

Among the powder consolidation processes, the recently widespread use of the Spark Plasma Sintering (SPS) technique has resulted in a considerable amount of literature and patents.[29,30] However, very few studies dealing with the applicability of this technique to the consolidation of polymers, more particularly PI, have been published so far. Omori et al.[23–26] reported that

Table I. Processing Conditions of PI Obtained by Powder Consolidation, as Reported in the Literature

Method	Heating rate (°C/min)	Temperature (°C)	Pressure (MPa)	Dwell time (min)	References
Hot-press molding			10 ($T < 315$°C)		
	8	340	25 ($T > 315$°C)	10	13
	2	300	27	60	4
	NS	315	10	120	14
	NS	370	40	75	15
	NS	380	40	75	16,17
	NS	380	20	60	18
Pressureless sintering	NS	NS	NS	NS	DuPont™ Vespel® SP[19]
Injection molding	NS	390	21	NS	DuPont™ Vespel® TP[20]
	NS	380–410	75–140	NS	DuPont™ Vespel® TP[21]
	NS	410–430	75–240	NS	DuPont™ Vespel® CF-TP[21]
	NS	380	10	NS	General Electric™ Ultem®-1000[22]
Spark Plasma Sintering	50	200–380	10–147	5	23–26
	NS	220–280	50	5	27,28
	NS	380	NS	5	5

the suitable SPS consolidation temperature and the mechanical properties are strongly dependent on the applied pressure. At 200°C, a pressure of 147 MPa was necessary to obtain a thermosetting PI with a full density (1440 kg/m^3) corresponding to Young's modulus of 4.40 GPa. PI was degraded by carbonization at a temperature above 300°C, for a pressure greater than 19.6 MPa, and then at a temperature higher than 230°C for a pressure of 39.2 MPa.

Tanaka et al.[27,28] developed PI-based composites by means of SPS for friction and wear applications. They filled PI samples with carbon or diamond particles in order to enhance the wear properties. The pressure was set at 50 MPa and the composites were sintered at 220°C. At higher sintering temperatures, some cracks were observed and the antiwear properties deteriorated. For space structure composites, Naskar et al.[5] used PI consolidated at 380°C by resistive heating. Rigid composites exhibiting voids and flaws were obtained. These defects were attributed to non-optimized consolidation conditions.

Although the feasibility of using the SPS method to consolidate PI was pointed out in the literature,[5,23–28] a lack of optimization of the SPS parameters and an insufficient understanding of the SPS consolidation mechanisms were highlighted. The sintering conditions (Table I) can vary according to the wide range of temperatures, pressures, and dwell times. Moreover, some parameters such as the temperature and pressure are interrelated, as demonstrated by Omori et al.[23–26] The principle of the SPS technology is that a pulsed electric current flows directly through a compaction die and a powder sample, while uniaxial loading is applied in parallel. If the powder is electrically insulating, only indirect heating by the die is generated. To obtain a homogeneous temperature distribution, the dimensions of the tools must be optimized. Based on the observations listed in Table I and on the conditions determined in a previous study (heating rate, SPS tool dimensions),[31] this work aims at studying the effects of the SPS processing parameters on the physical and structural characteristics of PI, as well as their influence on the mechanical properties of the resulting materials. A Design of Experiments (DOE) was implemented to study the influence of the temperature, pressure, dwell time, and cooling rate on the bulk properties of PI by applying the analysis of variance (ANOVA) method. The homogeneity of the mechanical properties of the sintered material was evaluated and the results were correlated with the polymer structure and fracture morphology by means of scanning electron microscopy (SEM) observations. Mechanisms associated to the PI densification were then determined.

EXPERIMENTAL

Polyimide

An amorphous PI raw powder (Evonik), granulated into agglomerates ranging from 400 to 800 μm was used. The average particle size of the powder is in the 1–10 μm range, as shown in Figure 1. The glass transition temperature (T_g) of this polymer and its theoretical density are, 320°C and 1380 kg/m^3, respectively.

Spark Plasma Sintering

Specimens were sintered by using an HP D 125 SPS facility from FCT Systeme GmbH (Rauenstein, Germany). The powder was weighed so as to obtain pellets of 10 mm in thickness and 30 mm in diameter at full densification. In all the experiments, the temperature was monitored and regulated by a K-thermocouple placed at a distance of 2 mm from the inner surface of the die.

Sintering was carried out under vacuum conditions at a heating rate of 10°C/min to ensure the temperature homogeneity in the die and punch assembly. A uniaxial pressure was applied at 250°C and increased gradually to reach the desired load in 2 min. The final pressure was maintained during the heating and

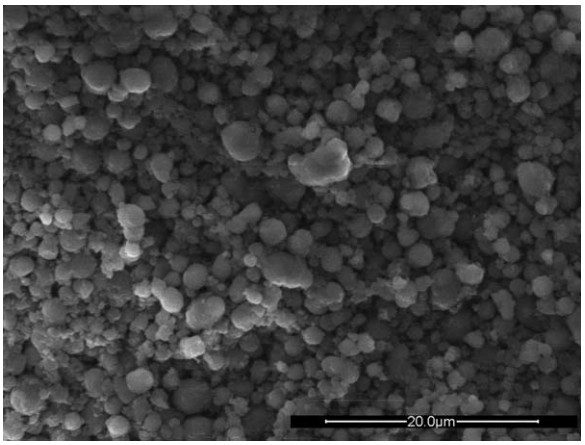

Figure 1. SEM image of the PI raw powder.

dwelling stages. Once the sintering temperature was reached, the sample was kept in these conditions for some time and then was gradually cooled down to 250°C. At this temperature, the uniaxial pressure was released in 2 min. Finally, free cooling was applied until room temperature was reached.

Design of Experiments

Experiments were designed based on a DOE study to understand the effects of various SPS processing parameters on the PI densification. The principle of this approach is to determine the subset of factors that exert the greatest impact on the set of responses relative to a given number of experimental measurements.[32,33] This method is used to find the critical factors that lead to improve a process. The influence of the processing conditions, including the temperature, pressure, and dwell time was investigated as their effects on the structural characteristics and mechanical properties of the materials obtained by powder metallurgy (P/M) was recognized in the literature (Table I). The effect of the cooling rate was added since this parameter might play a role in relieving residual stresses inside the material, as observed in polymer-based composites.[34,35] The different processing parameters (selected factors) and levels (values within a given range) are summarized in Table II. While all parameters are studied at two levels, the temperature is examined at three levels, as the latter appears to be the most significant parameter in the literature (Table I). The data analysis of the results was carried out using the Design-Expert® (version 8, State-Ease®) software with a response surface method (RSM) for process optimization. The 2FI model taking into account the *A*, *B*, *C*, *D* effects and *AB*, *AC*, *BC*, *BD* interactions was applied. The experimental responses were the density, Young's modulus *E*, the Shore D hardness, the maximum compressive strength σ_{max}, and the maximum compressive strain ε_{max}. The DOE approach was composed of 24 experiments. All the SPS cycles tested in this study are presented in Table II. The resulting responses were rounded to the significant digits by performing statistical calculations using standard deviation.

Analysis of Variance

The two-way ANOVA test was used as a statistical tool to determine the main effect contributions of the factors and also to identify whether there is a significant interaction effect between the factors by means of an *F*-test (*F* and *P* values).

A two-way ANOVA model composed of two factors *A* and *B*, having respectively *a* and *b* levels and a number of *ab* combinations, can be written following Eq. 1:

$$y_{ijk}=\mu+\alpha_i+\beta_j+\gamma_{ij}+\varepsilon_{ijk};\ \ \varepsilon_{ijk}\sim N\left(0,\sigma_{ij}^2\right);\quad k=1,2,\ldots,n_{ij};\ i=1,2,\ldots,a;\ j=1,2,\ldots,b \tag{1}$$

where y_{ijk} is the response, μ the grand mean, α_i and β_j are the *i*th and *j*th main effects of the factors *A* and *B* and γ_{ij} is the (*i*, *j*)th interaction effect between the factors *A* and *B*. The basic method of the two-way ANOVA test can be applied to our DOE study according to the method reported in the literature.[36]

Mean Calculation.

$$\bar{y}=\frac{1}{ab}\sum_{i=1}^{b}\sum_{j=1}^{a}y_{ij};\ \bar{y}_i=\frac{1}{a}\sum_{j=1}^{a}y_{ij};\ \bar{y}_j=\frac{1}{b}\sum_{i=1}^{b}y_{ij};\ \bar{y}=\frac{1}{a}\sum_{i=1}^{a}\bar{y}_i=\frac{1}{b}\sum_{j=1}^{b}\bar{y}_i \tag{2}$$

where $\bar{y}$ represents the mean value of the measurements.

Calculation of the Sum of Squares.

$$\sigma^2=\frac{\mathrm{SS}}{df} \tag{3}$$

where σ^2 is the variance, SS is the total sum of squared deviations from the mean, and *df* is the total degree of freedom corresponding to the total number of experiments minus one, i.e. 23 in our case.

$$\mathrm{SS}=\sum_{i=1}^{b}\sum_{j=1}^{a}\left(y_{ij}-\bar{y}\right)^2=\mathrm{SSA}+\mathrm{SSB}+\mathrm{SSE} \tag{4}$$

where SSA represents the sum of squared deviations caused by the factor *A*, SSB represents the sum of squared deviations caused by the factor *B*, and SSE represents the sum squared errors. SSA, SSB, and SSE can be obtained by using well-known equations.[36]

F-Test. First, the mean value of the sum squared deviations (MS) has to be calculated:

$$\mathrm{MSA}=\frac{\mathrm{SSA}}{a-1};\ \mathrm{MSB}=\frac{\mathrm{SSB}}{b-1};\ \mathrm{MSE}=\frac{\mathrm{SSE}}{(a-1)(b-1)} \tag{5}$$

Then, the *F*-value can be determined following the *F*-test:

Table II. SPS Processing Factors According to the Different Levels Examined in the PI Consolidation Study

Factors	Level 1	Level 2	Level 3
A—Temperature (°C)	290	320	350
B—Pressure (MPa)	40	100	-
C—Dwell time (min)	5	30	-
D—Cooling rate (°C/min)	5	20	-

$$F(A)=\frac{\mathrm{MSA}}{\mathrm{MSE}};F(B)=\frac{\mathrm{MSB}}{\mathrm{MSE}} \quad (6)$$

where F is the ratio of the variability between groups (MSA and MSB variances) to the variability within groups (MSE variance) that follows the Fisher–Snedecor distribution (F-distribution). For a given level α, the factor A has a significant effect on the test results if:

$$F(A) > F(\alpha)(a-1,(a-1)(b-1)) \quad (7)$$

This method was applied to each factor and the probability $P(F > F(\alpha))$ is called P-value. This analysis was carried out for a level of significance of 5%, i.e. for a level of confidence of 95% (P-value < 0.05).

Coefficient of Determination (R^2). R^2 indicates how well the experimental data fit the 2FI model. The most general definition can be written as:

$$R^2=1-\frac{\mathrm{SSE}}{\mathrm{SS}} \quad (8)$$

Characterization

The densities of the sintered specimens were determined by using the helium pycnometer method (Micromeritics AccuPyc 1330).

The Shore D hardness (Innovatest THS-210) measurements were performed at different locations in the thickness and the diameter of the samples.

Compression tests were conducted with a testing machine (Instron 5500 K9400) at a crosshead displacement rate of 1 mm/min to determine Young's modulus, the compressive strength, and compressive strain at break. The tests were carried out on specimens of 5 mm in diameter and thickness at three different positions in the sintered pellet, as reported in a previous article.[31]

The cryogenic fracture surfaces of the specimens before the compression tests and their fracture surfaces after the tests were coated with an Au conductive layer and were observed by SEM (FEI Quanta 400 and Zeiss DSM 982).

RESULTS AND DISCUSSION

Influence of the SPS Parameters on the Density

The density distribution presented in Table III for the 24 samples is narrow. Only three values, corresponding to the experiments performed at 290°C, are not included in the range between 1.36 and 1.39 $\times$ 10^3 kg/m^3. The F-test of the experimental results on the density (Table IV) show that A, B, and AB are significant model terms as they display a P-value < 0.05. The temperature and the pressure are the two parameters that have to be controlled to obtain fully dense PI pellets.

If C is set at 5 min and D at 5°C/min, the 2D response graph (RSM) of the AB interaction (Figure 2) explains how the density changes as a function of the temperature and of the pressure of SPS sintering cycles. At a given pressure in the range from 40 to 100 MPa, the density increases with the temperature. In the same way, at a given temperature between 290 and 350°C, the density improves when the pressure is increased. The maximum density (1.38 $\times$ 10^3 kg/m^3) is reached by raising both the pressure and the temperature. At 40 MPa, a fully dense PI pellet is obtained at a temperature close to 350°C. On the other hand, the dense PI sample is consolidated at a lower temperature around 325°C, when the pressure is set at 100 MPa. The interaction between the pressure and the temperature is clearly illustrated in Figure 2 and confirms the observations of Omori et al.[23–26]

The 2FI model applied to the PI density measurements presents a coefficient of determination $R^2=0.7284$. It shows that approximately 73% of the variance is explained by this regression. The dispersion is not totally solved by this model as other interactions such as ABC, included in the quadratic model, may also contribute to the density evolution. In this study, only the interactions between two factors were considered (2FI model).

Influence of the SPS Parameters on the Hardness

As in the case of the density results, the Shore D hardness measurement distribution is narrow with 22 values out of 24 in the 86–89 range (Table III). The F-test reported in Table V shows the significance of the A, B, and BC model terms. The temperature represents approximately half the contribution of the hardness results. The pressure and the interaction between the pressure and the dwell time represent 30 and 23% of the contribution, respectively. Once more, the temperature and the pressure are significant parameters that have to be controlled in order to obtain a maximum value of 89 for the Shore D hardness, very close to the reference value of 90 (PI hot-pressed by the powder supplier).

The effect of the pressure–time interaction is explained and illustrated by the 2D RSM graph reported in Figure 3, where the cooling rate is set at 20°C/min. At 290°C [Figure 3(a)], the increase in the pressure from 40 to 100 MPa and in the dwell time from 5 to 30 min results in the linear increase of the Shore D hardness which reaches the value of 88 for 100 MPa and 30 min. At 350°C [Figure 3(b)], the evolution of the hardness is not linear. A maximum value of 88.8 is achieved under consolidation conditions of either 100 MPa and 5 min or 40 MPa and 30 min. Therefore, a time gain of 25 min can be obtained by applying a higher pressure to get PI pellets with optimum hardness. This observation can be correlated with the density results since, at a given temperature, the density value increases when the pressure is raised.

The coefficient of determination $R^2=0.7242$, corresponding to the 2FI model, shows that approximately 72% of the variance is explained by this regression. The dispersion of the hardness values is not totally solved by this model. This observation can be attributed to the narrow distribution of the measurements, leading to a mean value very close to the experimental ones.

After measuring the hardness and density values, the mechanical results and, more precisely, Young's modulus and the compressive strength and strain are now presented.

Influence of the SPS Parameters on the Mechanical Properties Obtained by Compression Tests

The compression tests were only performed on PI samples densified at 320 and 350°C. All the pellets exhibited homogeneous mechanical properties at different locations, except for the

Table III. The 24 SPS Tests Carried Out by Means of the DOE Approach

	Factor *A*	Factor *B*	Factor *C*	Factor *D*	Response 1	Response 2	Response 3	Response 4	Response 5
Run	Temperature (°C)	Pressure (MPa)	Dwell time (min)	Cooling rate (°C/min)	Density (10^3 kg/m^3)	Shore D hardness	Young's modulus (GPa)	Compressive strength (MPa)	Compressive strain (%)
2	290	40	5	5	1.286	83.7	–	–	–
12				20	1.293	84.1	–	–	–
16			30	5	1.332	86.5	–	–	–
13				20	1.365	87.5	–	–	–
22		100	5	5	1.386	88	–	–	–
6				20	1.372	88	–	–	–
15			30	5	1.374	87	–	–	–
4				20	1.383	87.8	–	–	–
18	320	40	5	5	1.379	87.8	3.04	241	43.6
3				20	1.375	87.3	3.25	389	53.3
23			30	5	1.385	88.5	3.29	709	60.6
5				20	1.372	88.1	3.37	706	59.2
10		100	5	5	1.377	87.7	1.88	65	3.8
17				20	1.373	88.3	2.25	69	9.6
9			30	5	1.377	87.6	3.14	206	22.5
21				20	1.385	88	3.29	372	49.1
1	350	40	5	5	1.375	87.3	3.43	738	61.8
19				20	1.370	87.7	3.35	735	60.2
11			30	5	1.379	87.6	3.39	722	59.7
20				20	1.383	88.2	3.38	728	60.4
7		100	5	5	1.380	88.6	3.38	663	57.6
14				20	1.377	88.2	3.38	657	57.6
8			30	5	1.377	87.8	3.42	698	58.9
24				20	1.386	89	3.30	716	60.6

specimens sintered at 290°C that displayed low cohesion strength, for which it was not possible to carry out compression tests.

The *F*-tests reported in Table VI and relative to Young's modulus (E), to the compressive strength (σ_{max}) and to the

Table IV. RESULTS of the ANOVA Calculation Relative to the Density

Factors and interactions	*F*-value	*P*-value	Contribution (%)
A—Temperature	10.19	0.0071	37
B—Pressure	7.86	0.0149	29
C—Dwell time	3.00	0.1065	–
D—Cooling rate	0.10	0.7516	–
AB	9.42	0.0089	34
AC	1.64	0.2219	–
AD	0.16	0.6907	–
BC	1.78	0.2039	–
BD	0.027	0.8706	–
CD	0.63	0.4396	–

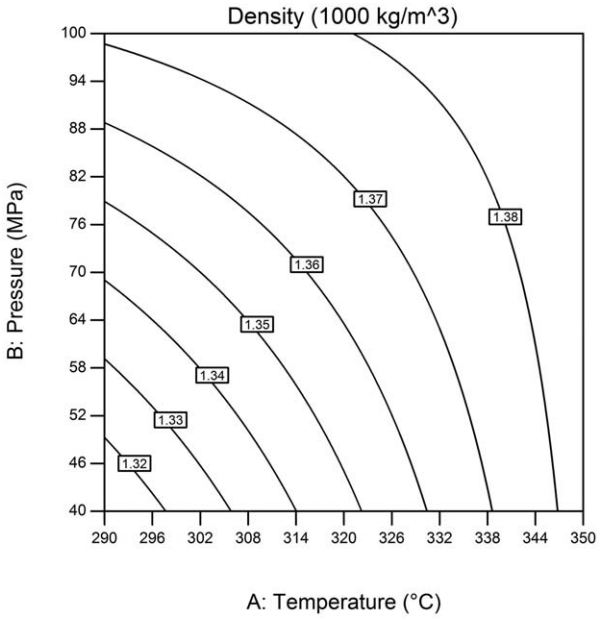

Figure 2. Evolution of the PI pellet density as a function of temperature and pressure.

Table V. Results of the ANOVA Calculation Relative to the Shore D Hardness

Factors and interactions	*F*-value	*P*-value	Contribution (%)
A—Temperature	11.86	0.0044	47
B—Pressure	7.64	0.0161	30
C—Dwell time	2.64	0.1280	-
D—Cooling rate	0.92	0.3540	-
AB	3.19	0.0971	-
AC	1.45	0.2492	-
AD	0.01	0.9205	-
BC	5.80	0.0315	23
BD	0.06	0.8071	-
CD	0.52	0.4820	-

maximum compressive strain (ε_{max}) reveal the significance of the factors *A*, *B*, and *C* and the interactions *AB* and *AC*. In the case of *E*, the interaction *AB* was deliberately added, as its *P*-value (0.0511) was very close to 0.05 (confidence of 95%). For all the mechanical properties, the factor that has the strongest impact is the temperature, with contributions equal to 33, 56, and 39% for *E*, σ_{max}, and ε_{max}, respectively. For *E*, the other contributions are fairly evenly distributed between the pressure, the dwell time, and the temperature–pressure and temperature–dwell time interactions. In contrast, the contributions for σ_{max} and ε_{max}, which correspond to properties at break, are distributed differently. The sum of the temperature and pressure contributions is 71% for σ_{max} and 64% for ε_{max}, indicating that only 29% of the contributions for σ_{max} and only 36% for ε_{max} are attributed to the dwell time and the interactions between temperature and pressure and between temperature and dwell time.

The optimum mechanical properties E=3.43 GPa, σ_{max}=738 MPa, and ε_{max}=61.8% were obtained by using the SPS method at a temperature of 350°C, a pressure of 40 MPa, and a dwell time of 5 min (Table III, Run 1). To our knowledge, these values are the highest ones reported in the literature,[1,2] obtained by sintering an unfilled thermoplastic PI material. While conventional sintering processes such as hot-press molding, powder injection molding, and free sintering require a few hours to obtain full density (Table I), the SPS method shows its potential for sintering advanced materials within a very short processing time. Figures 4–6 show 2D RSM graphs of the evolution of the mechanical properties as a function of pressure and temperature with a dwell time and a cooling rate set at 5 min and 5°C/min, respectively.

The three mechanical properties *E*, σ_{max}, and ε_{max} (Figures 4–6) exhibit the same evolution as a function of pressure and temperature. For a sintering pressure of 40 MPa, the *E*, σ_{max}, and ε_{max} values increase when the sintering temperature rises from 320°C to 350°C. However, when the sintering pressure is of 100 MPa at a given temperature, the *E*, σ_{max}, and ε_{max} values are lower than for a sample sintered at 40 MPa. The *C* factor and *AC* interaction, corresponding to the dwell time and to the temperature–dwell time interaction, respectively, show a significant contribution. At a given temperature and at 100 MPa, the increase in the dwell time leads to the enhancement of *E*, σ_{max}, and ε_{max}. As the strength of polymer interfaces is directly dependent on the interdiffusion of macromolecular chains (chain penetration depth, entanglements),[37,38] which is a function of time,[39,40] the observations can be correlated with this time dependence. Applying a high pressure of 100 MPa could affect and limit the interdiffusion of polymer chains that facilitates the interactions between grains and therefore the cohesion of the PI sample, particularly above the glass transition temperature T_g. Although Sauer and Pae[41,42] had formerly reported that the mechanical properties of cold-formed PI were improved by applying a high pressure, the counter-intuitive and negative effects of pressure on polymer interfaces at higher temperatures were observed latter by Wool et al.[43,44] They demonstrated that a minimum pressure is necessary to promote the intimate contact and the wetting of polymer chains, and by increasing this pressure, they pointed out the decrease in the fracture energy of

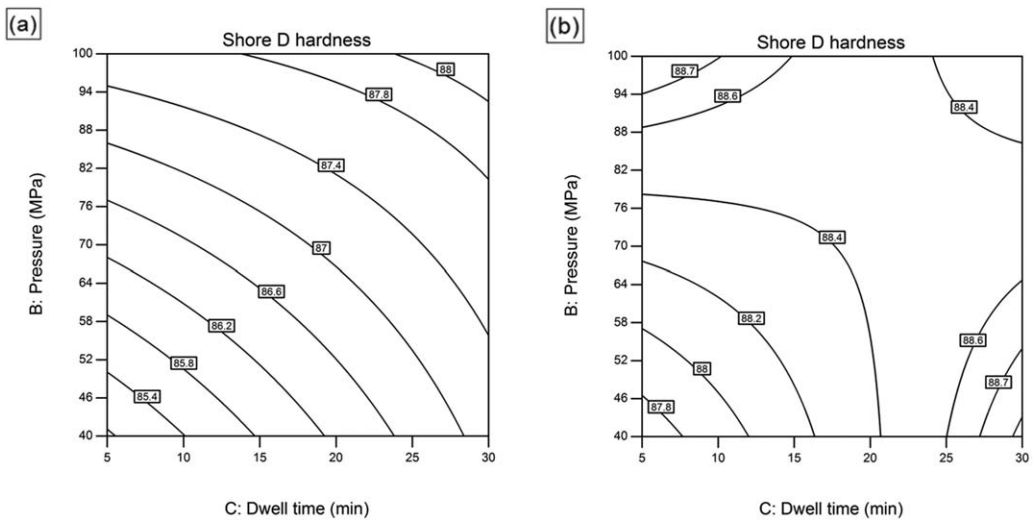

Figure 3. Evolution of the PI sample hardness as a function of pressure and dwell time at 290°C (a) and 350°C (b).

Table VI. Results of the ANOVA Calculation Relative to the Mechanical Properties

	Young's modulus			Compressive strength			Compressive strain at break		
Factors and interactions	*F*-value	*P*-value	Contribution (%)	*F*-value	*P*-value	Contribution (%)	*F*-value	*P*-value	Contribution (%)
A—Temperature	15.13	0.0115	33	103.06	0.0002	56	45.67	0.0011	39
B—Pressure	7.41	0.0416	16	28.39	0.0031	15	28.85	0.0030	25
C—Dwell time	8.23	0.0350	18	20.65	0.0061	11	10.41	0.0233	9
D-Cooling rate	0.45	0.5292	-	1.33	0.3009	-	2.58	0.1688	-
AB	6.51	0.0511	14	16.03	0.0103	9	23.01	0.0049	19
AC	9.03	0.0299	19	16.41	0.0098	9	9.18	0.0290	8
AD	1.24	0.3157	-	1.10	0.3407	-	2.38	0.1829	-
BC	4.47	0.0879	-	0.61	0.4680	-	2.57	0.1695	-
BD	0.05	0.8311	-	0.01	0.9113	-	1.05	0.3512	-
CD	0.19	0.6793	-	0.02	0.8893	-	0.28	0.6182	-

the interface. In a recent study of molecular dynamics simulation for the interdiffusion of polymer flow fronts flowing parallel to one another, Yokomizo et al.[45] observed that the time evolution of the weld interface thickness was hindered by shear flow. In our case, high pressures applied during the SPS process may similarly lead to interfacial shear stresses and limit the interdiffusion phenomena. As a result, the PI mechanical properties become lower when the pressure is increased.

The coefficients of determination R^2 of the E, σ_{max}, and ε_{max} regressions according to the 2FI model are of 0.9134, 0.9740, and 0.9618, respectively. More than 90% of the variance of the E value is explained by this regression, meaning that the model is suited to the experimental results. Furthermore, more than 95% of the variance of the σ_{max} and ε_{max} values is explained by this model. There is a very good agreement between this regression and the experimental data.

Correlation between the SPS Sintering Conditions and the PI Structure

SEM observations were made to correlate the SPS consolidation parameters with the material structure. As the cooling rate was demonstrated to have no effect on the density and on the mechanical properties of the PI specimens, only the influence of the temperature, pressure, and dwell time was considered for further discussion.

Effect of temperature. The cryogenic fracture micrographs taken before the compression tests for both samples sintered at 290°C [Figure 7(a)] and 350°C [Figure 7(b): $B = 40$ MPa, $C = 5$ min, $D = 5$°C/min] (Table III: Run 2 vs. Run 1) reveal that the

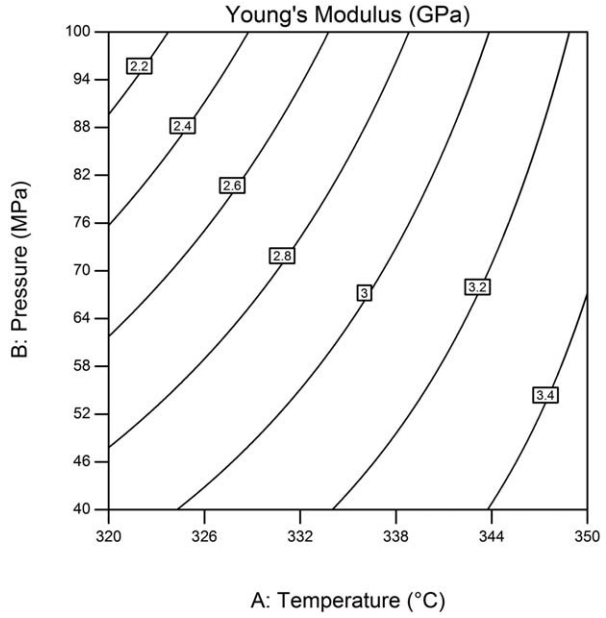

Figure 4. Young's modulus evolution for the PI specimens as a function of pressure and temperature.

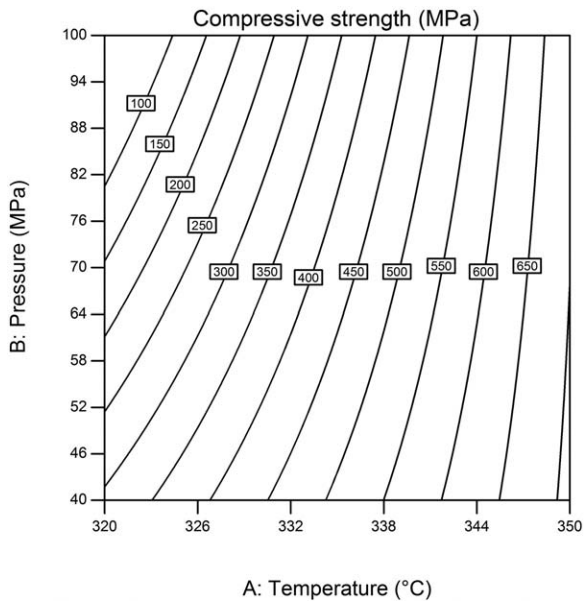

Figure 5. Compressive strength evolution for the PI specimens as a function of pressure and temperature.

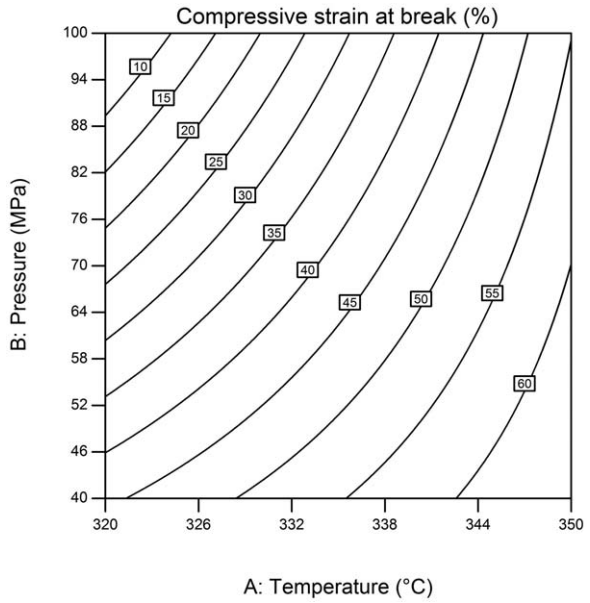

Figure 6. Evolution of the compressive strain at break for the PI specimens as a function of pressure and temperature.

initial structure of the powder is preserved with a particle size in the 1–10 μm range; grain boundaries can be observed. The microstructure observed at 320°C is the same as the one observed at 290°C.

Nevertheless, the strain at the grain boundaries is more pronounced at 350°C, meaning that there is a stronger cohesion between the sintered particles, while at 290°C the particles are just compacted. Above T_g, at 350°C, the mobility of the polymer chains is higher than at 290°C, leading to an increase in the interdiffusion of macromolecular chains at the interface between particles and, as a result, to a greater cohesion strength between them. Those observations are consistent with the compression test results which show that the PI sample consolidated at 350°C exhibits higher mechanical properties than at 290°C.

In Figure 8, the comparison of the fracture surfaces after the compression tests carried out on the specimens consolidated at 320°C and 350°C (corresponding to Table III: Run 18 vs. Run 1), shows a stratification of the polymer. The sample sintered at 320°C [Figure 8(a)] displays the initial structure of the powder with an intergranular fracture type, typical of a fragile material. However, for the PI pellet sintered at 350°C, the initial structure of the particles disappears and the SEM micrographs reveal a more ductile fracture with the presence of fibrils and stretched polymer particles. Moreover, Figure 8(b) shows microvoids appearing after the compression tests, which could correspond to residual closed porosity, causing cracks to occur and propagate. This difference in the types of fractures can be explained by the quality of the particle cohesion at the grain boundaries shown in Figure 7. Even though the temperature of 320°C is very close to the theoretical T_g, a temperature of 350°C is necessary to obtain optimum and maximum mechanical properties within a dwell time of 5 min.

Effect of Dwell Time. It is possible to counterbalance the influence of the temperature on the structure and on the mechanical properties by increasing the dwell time, as shown in Table III (Run 23 vs. Run 1). Mechanical properties close to the optimum and maximum ones obtained previously (see Influence of the SPS Parameters on the Mechanical Properties Obtained by Compression Tests) can be reached at 320°C, 40 MPa, and at a dwell time of 30 min. These results on mechanical properties (E=3.29 GPa, σ_{max}=709 MPa, ε_{max}=60.6%) can be correlated with the SEM observations reported in Figure 9.

The SEM micrograph (Figure 9) shows the same structure as for a sample sintered at 350°C for 5 min with the presence of fibrils and stretched polymer particles. The influence of the dwell time on the interdiffusion mechanisms and on the kinetics of the macromolecular chains can be clearly observed. As a result, the cohesion strength of the material consolidated at a temperature close to T_g is enhanced by a longer dwell time.

Effect of Pressure. The influence of the pressure was studied by setting the dwell time at 5 min and the cooling rate at 5°C/min. The specimens sintered at 320°C (Table III, Run 10) and 350°C (Table III, Run 7) and at a pressure of 100 MPa are compared in Figure 10.

The micrograph of the sample sintered at 320°C [Figure 10(a)] shows a mixture of the initial spherical structure of the powder (Figure 1) with the more cohesive structure obtained at 40 MPa

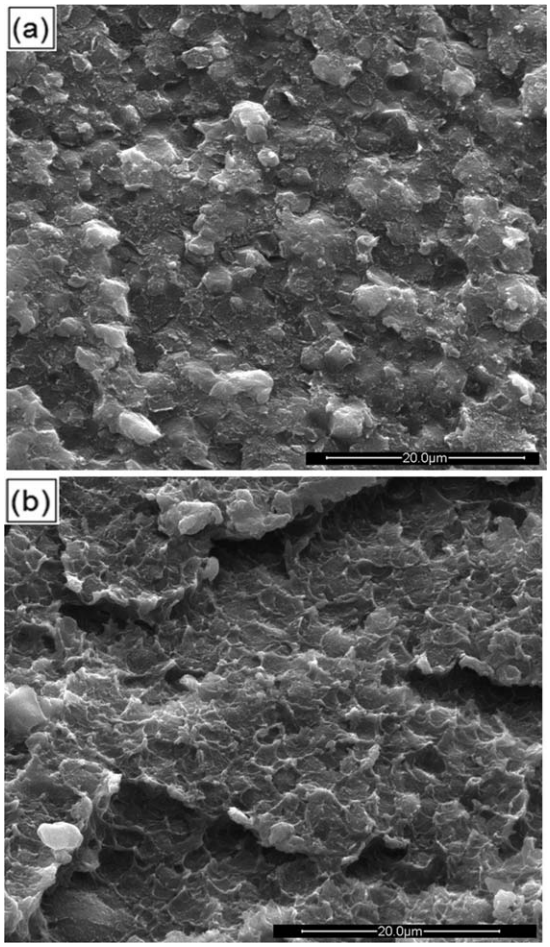

Figure 7. SEM micrographs of the cryogenic fracture surfaces of the PI samples sintered at 290°C (a) and 350°C (b).

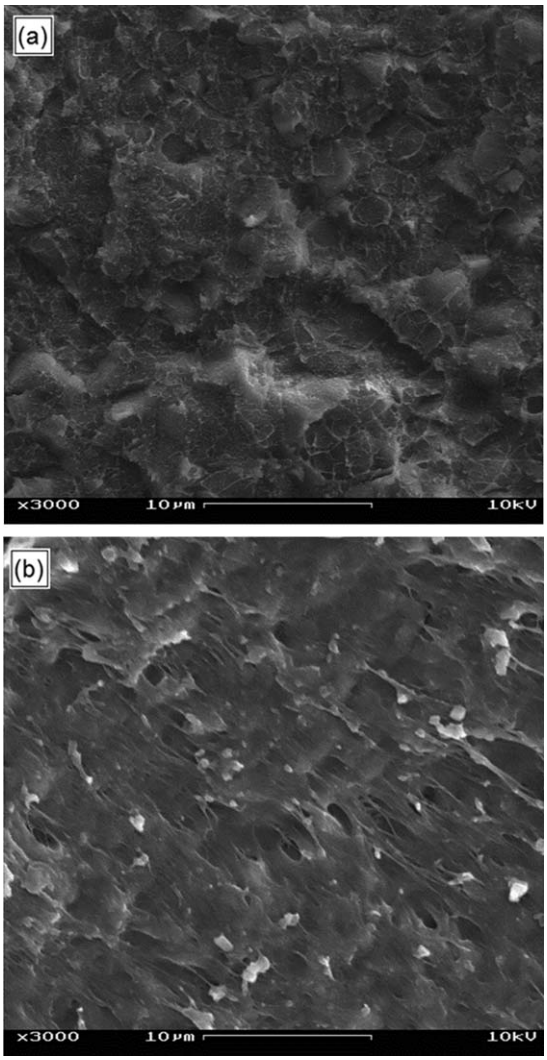

Figure 8. SEM micrographs of the fracture surfaces after the compression tests on the PI samples sintered at 320°C (a) and 350°C (b).

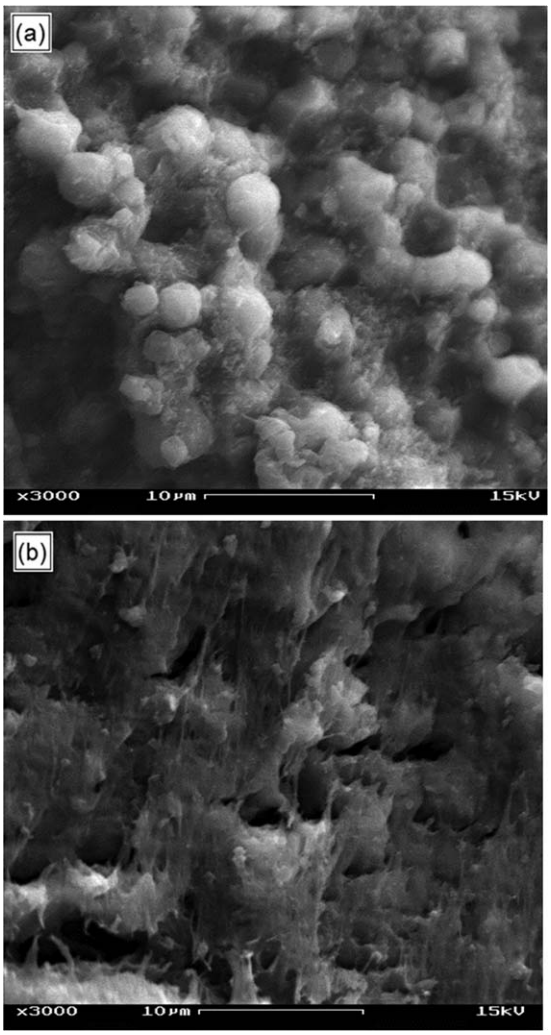

Figure 10. SEM micrographs of the fracture surfaces after the compression tests of the PI samples sintered at 320°C (a) and 350°C (b), at a pressure of 100 MPa.

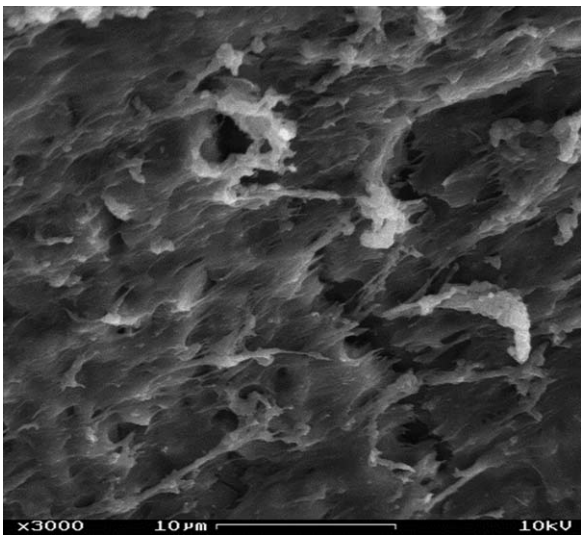

Figure 9. SEM micrographs of the fracture surface after the compression test on the PI sample sintered at 320°C and at a dwell time of 30 min.

[Figure 8(a)], which is in agreement with the very low mechanical properties achieved by the compression tests: E=1.88 GPa, σ_{max}=65 MPa, ε_{max}=3.8%. All the particles retain their spherical shape, no grain interfaces are formed, which means that the intergranular cohesion strength is very low. At a high pressure of 100 MPa (Figure 10), the agglomerates are disaggregated and the particles are not strongly bonded together, in comparison with Figure 8(a) where the pressure was set at 40 MPa.

At a sintering temperature of 350°C, the mobility of the polymer chains is higher than at 320°C and leads to a better interdiffusion of the macromolecular chains at the interface between the particles, even at a high pressure. Above T_g, the local heating due to the friction between particles could counterbalance their limited motion induced by the high pressure. Consequently, the polymer material can be observed to fibrillate and stretch after the compression tests [Figure 10(b)]. However, compared to a specimen sintered at 40 MPa [Figure 8(b)], the density of fibrils is lower for a pellet sintered at 100 MPa. This observation is consistent with the lower mechanical properties

achieved (E=3.38 GPa, σ_{max}=663 MPa, and ε_{max}=57.6%) when the pressure is increased.

CONCLUSION

In order to optimize the PI properties, the effects of the consolidation parameters involved in SPS were investigated. A DOE approach combined with an analysis of variance showed the significance of some parameters and of their interactions on the physical and mechanical properties of the sintered specimens. The temperature, the pressure, and their interaction are significant factors that have an influence on the density of a PI sample obtained by the SPS method. The temperature, the pressure and the pressure–dwell time interaction are the major parameters ensuring the maximum value of hardness. Finally, the temperature, the pressure, the dwell time, and the temperature–pressure and temperature–dwell time interactions are the conditions that contribute most to the final values of Young's modulus and to the compressive strength and strain and that have the maximum influence on them. Thanks to this procedure, a high-performance PI material with advanced and controlled mechanical properties (E=3.43 GPa, σ_{max}=738 MPa, and ε_{max}=61.8%) was sintered at 350°C and 40 MPa and at a dwell time of 5 min by using the SPS technique.

The study of the structure combined with the results on the mechanical properties allowed us to highlight that the interdiffusion of the macromolecular chains is the main mechanism occurring during the sintering of the PI. The achievement of cohesive grain boundaries is linked to the interdiffusion kinetics. Finally, the cohesion of the material is strongly dependent on the quality of the interfaces formed between the particles.

This material may be considered in the transportation field as structural material for light weighting applications.

ACKNOWLEDGMENTS

The authors thank the Direction Générale de l'Armement (DGA) for funding this research through the Ph.D. grant awarded to M. Schwertz.

REFERENCES

1. Sroog, C. E. *Prog. Polym. Sci.* **1991**, *16*, 561.
2. Liaw, D.-J.; Wang, K.-L.; Huang, Y.-C.; Lee, K.-R.; Lai, J.-Y.; Ha, C.-S. *Prog. Polym. Sci.* **2012**, *37*, 907.
3. Strunskusand, Y.; Grunze, M.; Crosh, M.; Mittal, K., Eds. *Polyimides—fundamentals and applications*; New York: Marcel Dekker: **1994**; p 187.
4. Livengood, B. P.; Chalmers, T. M.; Gu, Y.; Zhang, Y.-D.; Harris, F. W.; Cheng, S. Z. D. *Thermochim. Acta* **1994**, *243*, 115.
5. Naskar, A. K.; Edie, D. D. *J. Compos. Mater.* **2006**, *40*, 1871.
6. Ree, M.; Shin, T. J.; Kim, S. I.; Woo, S. H.; Yoon, D. Y. *Polymer* **1998**, *39*, 2521.
7. Yu, J.; Ree, M.; Shin, T. J.; Wang, X.; Cai, W.; Zhou, D.; Lee, K. W. *Polymer* **2000**, *41*, 169.
8. Spassova, E. *Vacuum* **2003**, *70*, 551.
9. Saeed, M. B.; Zhan, M. S. *Eur. Polym. J.* **2006**, *42*, 1844.
10. Deligoz, H.; Yalcinyuva, T.; Ozgumus, S.; Yildirim, S. *Eur. Polym. J.* **2006**, *42*, 1370.
11. Meng, X.; Huang, Y.; Yu, H.; Lv, Z. *Polym. Degrad. Stab.* **2007**, *92*, 962.
12. Chou, W.-J.; Wang, C.-C.; Chen, C.-Y. *Polym. Degrad. Stab.* **2008**, *93*, 745.
13. Cai, H.; Yan, F. Y.; Xue, Q. J.; Liu, W. M. *Polym. Test.* **2003**, *22*, 875.
14. Xie, W.; Pan, W.-P.; Chuang, K. C. *Thermochim. Acta* **2001**, 367, *143*.
15. Wang, Q. H.; Zhang, X. R.; Pei, X. Q. *Mater. Des.* **2010**, *31*, 3761.
16. Zhang, X.; Pei, X.; Wang, Q. *Mater. Chem. Phys.* **2009**, *115*, 825.
17. Zhang, X. R.; Pei, X. Q.; Wang, Q. H. *Mater. Des.* **2009**, *30*, 4414.
18. Zhao, G.; Hussainova, I.; Antonov, M.; Wang, Q.; Wang, T. *Wear* **2013**, *301*, 122.
19. Samyn, P.; Schoukens, G.; Quintelier, J.; De Baets, P. *Tribol. Int.* **2006**, *39*, 575.
20. Samyn, P.; Quintelier, J.; Schoukens, G.; De Baets, P. *Wear* **2008**, *264*, 869.
21. Samyn, P.; Schoukens, G. *Mater. Chem. Phys.* **2009**, *115*, 185.
22. Yudin, V. E.; Otaigbe, J. U.; Gladchenko, S.; Olson, B. G.; Nazarenko, S.; Korytkova, E. N.; Gusarov, V. V. *Polymer* **2007**, *48*, 1306.
23. Omori, M.; Okubo, A.; Kang, G. H.; Hirai, T. In Functionally Graded Materials 1996; Ichiroand, S., Yoshinari, M., Eds.; Elsevier Science B.V.: Amsterdam, **1997**; p 767.
24. Omori, M.; Okubo, A.; Gilhwan, K.; Hirai, T. *J. Mater. Synth. Process.* **1997**, *5*, 279.
25. Omori, M. *Mater. Sci. Eng. A* **2000**, *287*, 183.
26. Omori, M. In 3rd International Symposium on Structural and Functional Gradient Materials, Switzerland, **1994**, p 667.
27. Tanaka, A.; Umeda, K.; Yudasaka, M.; Suzuki, M.; Ohana, T.; Yumura, M.; Iijima, S. *Tribol. Lett.* **2005**, *19*, 135.
28. Tanaka, A.; Umeda, K.; Takatsu, S. *Wear* **2004**, *257*, 1096.
29. Grasso, S.; Sakka, Y.; Maizza, G. *Sci. Technol. Adv. Mater.* **2009**, *10*, 1.
30. Munir, Z. A.; Quach, D. V.; Ohyanagi, M. *J. Am. Ceram. Soc.* **2011**, *94*, 1.
31. Schwertz, M.; Lemonnier, S.; Barraud, E.; Carradò, A.; Vallat, M.-F.; Nardin, M. *J. Appl. Polym. Sci.* **2014**, *131*, 9389.
32. Aman, Y.; Garnier, V.; Djurado, E. *Int. J. Appl. Ceram. Technol.* **2010**, *7*, 574.
33. Enneti, R. K.; Carney, C.; Park, S.-J.; Atre, S. V. *Int. J. Refract. Met. Hard Mater.* **2012**, *31*, 293.
34. Gao, S.-L.; Kim, J.-K. *Compos. A* **2000**, *31*, 517.

35. Beehag, A.; Ye, L. *Appl. Compos. Mater.* **1995**, *2*, 135.
36. Fisher, R. Statistical Methods for Research Workers; Hafner Publishing Company: New York, **1973**.
37. Kausch, H. Polymer Fracture; Springer: Berlin-Heidelberg, **1978**.
38. Wool, R. P. Polymer Interfaces: Structure and Strength; Hanser Publishers: Munich, New York, **1995**.
39. Rouse, P. E. J. *J. Chem. Phys.* **1953**, *21*, 1272.
40. Gennes, P. G. D. *J. Chem. Phys.* **1971**, *55*, 572.
41. Sauer, J.; Pae, K.; Bhateja, S. *J. Macromol. Sci. Phys. B* **1973**, *8*, 631.
42. Sauer, J.; Pae, K. *Colloid Polym. Sci.* **1974**, *252*, 680.
43. Wool, R. P.; Yuan, B. L.; McGarel, O. J. *Polym. Eng. Sci.* **1989**, *29*, 1340.
44. Wool, R. P.; Willett, J. L.; McGarel, O. J.; Yuan, B. L. *Abstr. Pap. Am. Chem. Soc.* **1987**, 194, 175-POLY.
45. Yokomizo, K.; Banno, Y.; Kotaki, M. *Polymer* **2012**, *53*, 4280.